NANO LETTERS

2008
Vol. 8, No. 9
3017-3022

Coupled Electrooxidation and Electrical Conduction in a Single Gold Nanowire

Chengxiang Xiang,[†] Aleix G. Güell,[‡] Matthew A. Brown,[†] Jung Yun Kim,[†] John C. Hemminger,[†] and Reginald M. Penner*,[†]

Department of Chemistry, University of California, Irvine, California 92697-2025, and Department of Physical Chemistry, University of Barcelona, Marti i Franques 1, 08028, Barcelona, Spain

Received July 16, 2008; Revised Manuscript Received August 3, 2008

ABSTRACT

The resistance, *R*, of single gold nanowires was measured in situ during electrooxidation in aqueous 0.10 M sulfuric acid. Electrooxidation caused the formation of a gold oxide that is approximately 0.8 monolayers (ML) in thickness at +1.1 V vs saturated mercurous sulfate reference electrode (MSE) based upon coulometry and ex situ X-ray photoelectron spectroscopic analysis. As the gold nanowires were electrooxidized, *R* increased by an amount that depended on the wire thickness, ranging from $\Delta R/R_{0.10V} = 14\%$ for a 63 nm (h) × 200 nm (w) wire to 57% for an 18 nm (h) × 95 nm (w) wire at +1.1 V. These nanowires were millimeters in total length, but just 46 μm lengths were exposed to the electrolyte solution. The oxidation process and the accompanying increase in *R* were reversible: Reduction of the oxide at +0.10 V resulted in recovery of the reduced wire *R* except for a small resistance offset caused by the dissolution of ≈0.4 ML of gold during each oxidation/reduction cycle. The measured increase in *R* during oxidation exceeds by a factor of 4 the predicted increases in *R* associated with the reduction in cross-sectional area of the nanowire and the expected decrease in the specular scattering parameter, *p*, at the gold−oxide interface at wire surfaces. We propose that this anomalous increase in *R* is caused by infiltration of the oxide into the nanowire at grain boundaries.

Copper, silver, nickel, and other coinage metals have thermodynamically stable oxides that spontaneously form on the surfaces of these metals in moist air.[1] The influence of these oxide layers on transport through nanowires composed of these metals has not been investigated to our knowledge. Gold does not have a thermodynamically stable oxide,[1] but it provides a useful test system for investigations of the effect of oxidation on electrical conduction because an oxide layer can be reversibly formed on a gold surface by electrooxidation in acid electrolyte. For potentials negative of +2.2 V versus a saturated mercurous sulfate electrode (MSE), this oxide layer has a composition and thickness that depend only on the applied potential.[2,3] In this Letter we report the surprising results of experiments in which we measure the electrical resistivity of potentiostatically controlled gold nanowires that are immersed in dilute sulfuric acid.

This relationship between the composition and thickness of a gold oxide and the applied potential has been established by Bonzel and co-workers[3] who used ex situ X-ray photoelectron spectroscopy (XPS) in conjunction with coulometry to map the composition of a single crystalline gold surface in 1 M sulfuric acid as a function of the applied potential. They concluded the following: (1) From 0.64 to 0.84 V vs MSE ($E_{MSE} = 0.640$ V vs E_{NHE}), OH^- is adsorbed culminating in the formation of a monolayer of adsorbed OH^- at 0.84 V. (2) At potentials positive of 0.84 V, adsorbed OH^- is converted into $Au(OH)_3$. A complete monolayer of $Au(OH)_3$ is present at 1.05 V, and a second monolayer is completed at ≈1.35 V. (3) At still more positive potentials up to 2.2 V, $Au(OH)_3$ is converted into AuOOH. A bulk, three-dimensional layer of AuOOH forms on the gold surface at potentials above 2.2 V. Here, we investigate the effect of an oxide layer that is produced at an applied potential of 1.1 V vs MSE. At this potential, Bonzel and co-workers predict that just one complete monolayer of $Au(OH)_3$, in addition to adsorbed water, is present at the gold surface.[3] Estimates of its thickness by in situ ellipsometry are in the 4−6 Å range.[4−6]

How can the formation of $Au(OH)_3$ be expected to affect the electrical resistance, *R*, of a gold nanowire? Two effects must be taken into consideration in this calculation: First, the cross-sectional area of the nanowire, *A*, is reduced by the conversion of gold into gold hydroxide, $Au(OH)_3$, an insulator. Since the resistance of the nanowire is $R = \rho L/A$ where ρ is the resistivity of gold and *L* is the electrically isolated wire length, *R* is inversely proportional to *A*. The reduction in *A* induced by the formation of a surface oxide can be estimated based upon the prior work of Bonzel[3] in combination with our own XPS measurements of the

* Corresponding author.
[†] University of California.
[‡] University of Barcelona.

10.1021/nl8021175 CCC: $40.75
Published on Web 08/20/2008

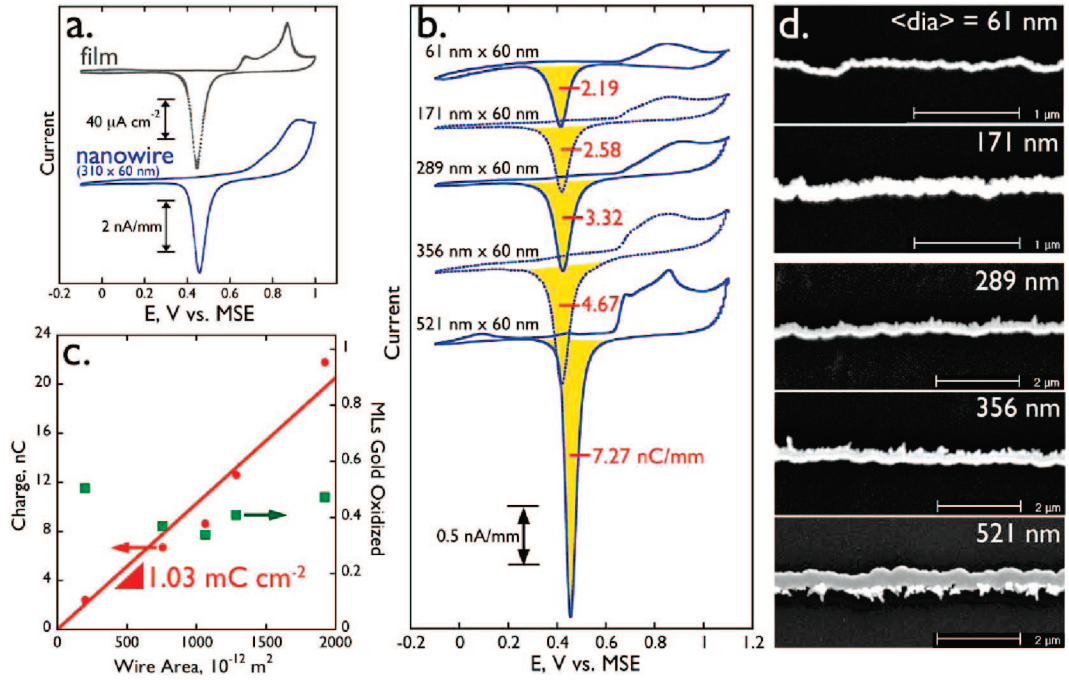

Figure 1. (a) Comparison of the cyclic voltammogram (CV) for an evaporated gold film in 0.10 M H_2SO_4 at a scan rate of 20 mV/s (top) and a gold nanowire in the same solution and scan rate. (b) CVs at five gold nanowires with the indicated dimensions. The charge associated with the oxide reduction wave, Q_{ox}, is indicated for each. The immersed wire lengths varied from 1 to 3 mm. (c) Plots of the charge, Q_{ox} versus wire area (red data). The slope of this plot yields 0.429 MLs of gold oxidized assuming rf = 4.0. Also shown are direct calculations of the number of gold monolayers oxidized (green data) for each of the five nanowires probed in (b). (d) SEM images of the five gold nanowires probed in (b).

oxidation layer thickness on our nanowire. Second, the specularity of electron scattering, p, is reduced also contributing to an increase in the resistance of the oxidized wire. The specularity parameter can vary between limits of $p = 1$, corresponding to pure specular scattering in which all surface scattering events conserve momentum, and $p = 0$, corresponding to fully diffuse scattering.

Although we are aware of no studies of the effect of oxidation on either metal films or nanowires, the effect on the resistance of metal films of the addition of "superimposed layers" of various other materials has been investigated. Chopra and Randlett[7] studied the effect of the addition of layers of Ni/Fe alloys, SiO, and germanium on the resistivity of silver, gold, copper, and aluminum films finding that all three materials caused an increase in the resistance of films of these metals. The largest $\Delta R/R_0$ values were 23% for 2 nm SiO layers on silver films with a thickness of 1−2 nm. Analogous experiments for SiO on gold yielded smaller $\Delta R/R_0$ in the 12% range,[7] but subsequent work on this system[8,9] produced $\Delta R/R_0$ values of ≈20%. Other metal−overlayer systems have been studied,[10] and in all cases, the imposition of an overlayer causes an increase in the resistance of the metal film. This increased resistance is attributed either to a reduction in p or to the emergence of a new and so far unspecified dissipation mechanism associated with the overlayer.[7−15]

On the basis of the results of these "two layer" experiments, we expect that the growth of an oxide layer on a gold nanowire will also cause a reduction in p, contributing to an overall increase in R. The magnitude of the change in p can be estimated as follows. The electrical resistivity of copper[16−19] and tungsten[20] nanowires with a rectangular cross section has been reported by Steinhogl and co-workers. These workers derived an equation[17,19] that relates wire resistivity, ρ, to its dimensions, the temperature-dependent bulk resistivity of the metal, ρ_0, and three additional parameters: the grain diameter, d, the specularity parameter, p, which is the fraction of surface scattering events that preserve momentum, from Fuchs−Sondheimer theory,[21,22] and R_c, the "reflectivity coefficient", which is the fraction of electrons that are scattered by the potential barrier presented by grain boundaries, from Mayadas−Shatzkes theory.[23]

$$\rho = \rho_0\left\{\frac{1}{3}\Big/\left[\frac{1}{3} - \frac{\alpha}{2} + \alpha^2 - \alpha^3 \ln\left(1 + \frac{1}{\alpha}\right)\right] + \frac{3}{8}C(1-p)\frac{1+\mathrm{AR}}{\mathrm{AR}}\frac{\lambda}{w}\right\} \quad (1)$$

with

$$\alpha = \frac{\lambda}{d}\frac{R_c}{1-R_c} \quad (2)$$

Other parameters in eqs 1 and 2 are w, the nanowire width, AR, its aspect ratio (AR = height/width), λ, the electron mean free path, taken to be 40 nm at room temperature,[24] and C is a constant that has a value of 1.2 for wires with a rectangular cross section.[19]

Equations 1 and 2 were used to calculate the resistance of the gold nanowires as a function of p and for values of R (=0.848) and d (=70 nm) that were obtained from a prior investigation of the temperature-dependent resistance and structure of single gold nanowires prepared by the LPNE method.[25] In that work, we concluded that the mean grain diameter deduced from the resistivity measurement is close

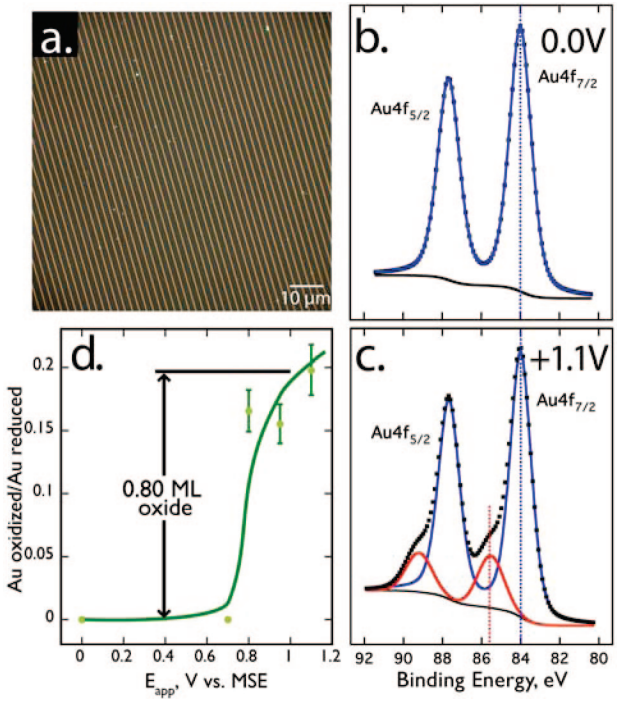

Figure 2. (a) Array of gold nanowires (400 nm (w) × 60 nm (h)), deposited at 2 μm pitch on glass, investigated by X-ray photoelectron spectroscopy (XPS). (b) Narrow scan XP spectrum of the gold 4f region for freshly prepared gold nanowires that were equilibrated at +0.0 V vs MSE in 0.10 M H_2SO_4 prior to emersion. This spectrum shows a binding energy of 84.0 eV for the $4f_{7/2}$ peak, characteristic of clean, elemental gold. (c) XP spectrum of the gold 4f region for nanowires that were electrooxidized at +1.1 V vs MSE. Deconvolution peak fitting of the shoulder on the high energy side of the elemental gold peaks (red curve) reveals the formation of an oxidized gold species with a binding energy of 85.6 ± 0.1 eV assigned to $Au(OH)_3$. (d) Plot of the gold intensity ratio between the peak assigned to $Au(OH)_3$ peak and that of elemental gold for nanowires equilibrated at five potentials: 0.0, 0.7, 0.8, 1.0, and 1.1 V vs MSE. The solid line provides a guide to the eye only.

to the actual grain dimensions measured by microscopy and X-ray diffraction. This means that the gold nanowires prepared by LPNE have a temperature-dependent resistance that is approximately correct for their known width and height, the measured grain diameter, and the known mechanisms of dissipation in nanoscopic metal wires.

Gold nanowires were prepared on glass surfaces using the lithographically patterned nanowire electrodeposition (LPNE) method.[26,25] These nanowires had a rectangular cross section with width and height dimensions that varied from 18 to 63 nm (h) and 95 to 220 nm (w). The voltammetry of single gold nanowires was measured by immersing a 1−3 mm length of nanowire, with a silver contact covered by epoxy at one end of the nanowire, into the sulfuric acid solution. Voltammograms for nanowires and evaporated gold films (Figure 1a) are qualitatively similar, both showing the onset of gold oxidation at +0.6−0.7 V vs MSE and rereduction of the oxide at +0.45 V; however the onset of oxidation for the nanowire is far more gradual, the peaks broader, and the current envelope less structured than that of the film which shows oxidation waves at +0.67 and +0.87 V. For the smallest nanowires examined here, the reduction wave occurs

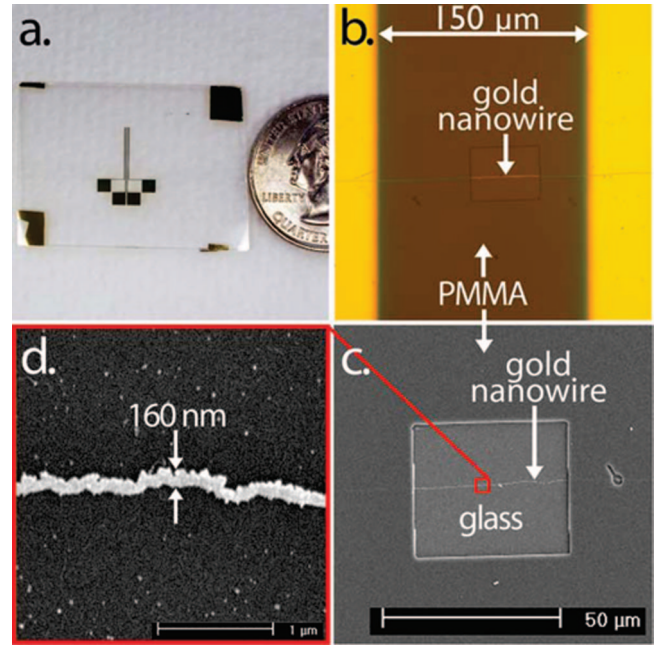

Figure 3. (a) Photograph of the four-point probe used to measure the resistance of a potentiostatically controlled gold nanowire in sulfuric acid. (b) Optical micrograph showing edges of inner two gold electrodes, separated by 150 μm, and a gold nanowire spanning these electrodes. The entire region shown is covered with a poly(methyl methacrylate) (PMMA) layer of thickness 400 nm, except for a rectangular window (width 46 μm) formed by electron beam writing at the center of the image. A section of this nanowire is exposed to the solution through this window. (c) Scanning electron micrograph (SEM) showing the gold nanowire through the window in the PMMA resist. (d) Higher magnification SEM image of the gold nanowire exposed within this window.

at a potential that is 10−15 mV more negative than that for bulk gold films, and a shift toward the bulk value is apparent for the largest nanowires (Figure 1b). This reduction wave encompasses the charge, Q_{ox}, associated with the rereduction of the oxide and Q_{ox} increases in direct proportion to the wetted surface area of the gold nanowire (Figure 1c). The slope of this plot (1.03 mC cm^{-2}) can be used to estimate the thickness of the oxide layer formed on the gold surface as follows: The charge associated with the conversion of one monolayer (ML) of gold atoms to Au^{3+} equals 0.60 mC/(ML cm^2).[27] The actual, microscopic area of these gold nanowires, A_{actual}, is larger than their geometric surface areas ($A_{geo} = (2h + w) \times$ length) by the "roughness factor", rf = A_{actual}/A_{geo}.[2] For example, Bonzel assumed an rf for single crystalline gold surfaces of 2.0,[3] whereas Juodkazis et al. used an rf of 3.7 for polycrystalline gold.[28] An additional source of roughness for our nanowires, not present in films, is the nanowire nonlinearity, and this justifies the use of a somewhat larger rf = 4.0, but this estimate is subject to considerable uncertainty and it could be higher resulting in a lower estimated oxide layer thickness. Using rf = 4.0, we obtain (1.03 mC/cm^2 × 0.25 cm_{geo}^2/cm_{actual}^2)/0.60 mC/(ML cm^2) = 0.429 ML Au^{3+}. As already indicated above, prior XPS studies show that this Au^{3+} presents as $Au(OH)_3$ at the gold surface but the molar volume, V_M, of this compound is not known. If we assume that the density of $Au(OH)_3$ equals that of Au_2O_3 (6.0 g/cm^3),[4] we calculate a V_M = 41.3 cm^3/

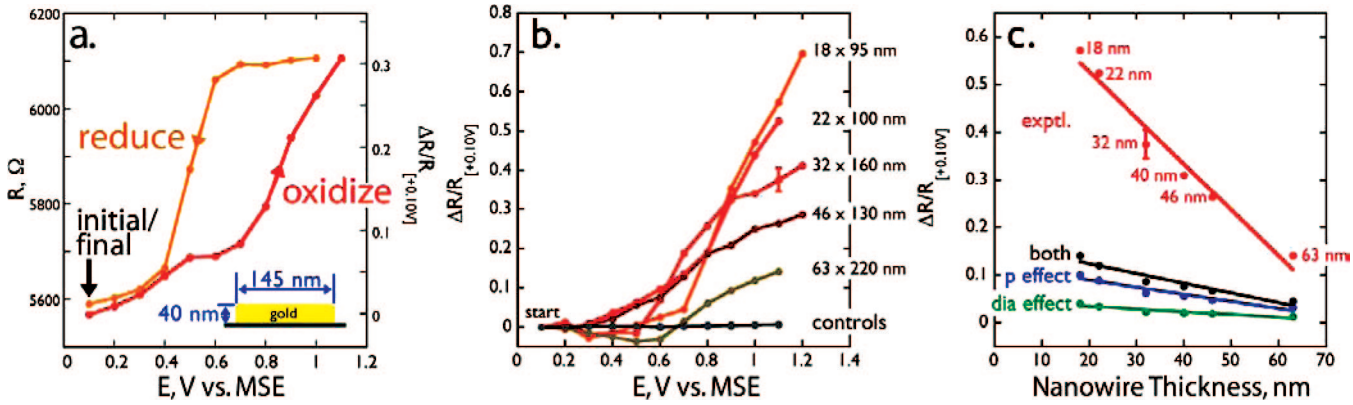

Figure 4. (a) Resistance, R, vs E_{app} for a 40 × 145 nm gold nanowire in 0.10 M H_2SO_4. The change in resistance, normalized by the resistance at +0.10 V, $\Delta R/R_{0.1V}$, is plotted at right. The hysteresis seen in this experiment reflects the intrinsic hysteresis of the surface electrochemistry, as seen for example in the cyclic voltammetry of Figure 1a. The initial and final potentials were both +0.10 V vs MSE. (b) $\Delta R/R_{0.1V}$ vs E_{app} for the oxidation of five other gold nanowires. (c) Plot of $\Delta R/R_{0.1V}$ evaluated at +1.1 V vs MSE vs height for the six nanowires in (a) and (b) (red trace). Also plotted are the calculated resistance change caused by the constriction in the wire diameter ($(\Delta R/R_{red})_{dia}$ in Table 1, green trace) and the change in p from 0.38 to 0.0 as calculated using eqs 1 and 2 ($(\Delta R/R_{red})_{p=0.38}$, blue trace) as well as the sum of these two contributions ($(\Delta R/R_{red})$, black trace).

Table 1. Electrooxidation-Induced Resistance Changes for Gold Nanowires and a Comparison with Theoretical Predictions

	experimental values			calculated values					
wire $h \times w$ (nm × nm)	A R_{red}[a] (kΩ)	B R_{ox}[b] (kΩ)	C $\Delta R/R_{red}$[c]	D $(\Delta R/R_{red})_{dia}$[d]	E $(\Delta R/R_{p=0.38})$[e]	F R/R_{red}[f]	G $R_{c,eff}$[g]	H x[h]	I oxide infiltration[i] (nm)
18 × 95	36.1	42.5	0.57	0.0395	0.0807	0.12	0.8985	0.332	5.98
22 × 101	24.0	27.9	0.52	0.0336	0.0661	0.10	0.8961	0.316	6.96
32 × 159	5.02	5.61	0.38	0.0223	0.0477	0.071	0.8860	0.250	7.99
40 × 145	5.56	6.11	0.31	0.0197	0.0414	0.062	0.8799	0.210	8.40
46 × 130	5.04	5.45	0.26	0.0188	0.0382	0.058	0.8749	0.177	8.13
63 × 220	1.38	1.45	0.14	0.0126	0.0284	0.041	0.8620	0.092	5.80

[a] R_{red} measured at +0.10 V vs MSE. [b] R_{ox} measured at +1.10 V vs MSE. [c] $\Delta R/R_{red} = (R_{ox} - R_{red})/(0.31R_{red})$ where 0.31 is the fraction of the electrically isolated length of the nanowire that was exposed to the H_2SO_4 electrolyte. [d] $(\Delta R/R_{red})_{dia}$ is calculated based upon a ΔR caused by the conversion of 0.5 nm of gold into a nonconductive gold oxide. [e] $(\Delta R/R_{p=0.38})_{dia}$ is calculated based upon a ΔR caused by a change in p from 0.38 to 0.0 (purely diffuse surface scattering). [f] $(\Delta R/R_{red})_{dia}$ is the total ΔR caused both by the change in p to 0.0 and by the reduction in diameter of the nanowire by the oxide. [g] The effective value of R_c necessary to produce the experimentally measured $\Delta R/R_{red}$. [h] The root of the equation: $R_{c,eff} = (1 - x)(0.848) + x(1.0)$ where 0.848 is the experimentally measured R_c for reduced gold nanowires, $R_c = 1.0$ is assumed to apply at oxidized grain boundaries within the nanowire, and x is the fractional cross section of the nanowire over which grain boundaries are oxidized. [i] Estimate of the mean infiltration depth of the oxide into grain boundaries at the surface of the nanowire, calculated as the product of x and the wire height (nm).

mol, and this translates into a layer thickness of 3.4 Å or ≈0.8 ML of oxide.

To identify the oxide produced by the electrooxidation of nanowires (e.g., Figure 1), we measured the X-ray photoelectron spectra of nanowire arrays equilibrated at applied potentials of 0, 0.7, 0.8, 1.0, and 1.1 V vs MSE. These arrays consisted of thousands of linear gold nanowires 400 nm (w) × 60 nm (h) deposited using LPNE at 2 μm pitch on a glass surface (Figure 2a). Nanowire arrays were first equilibrated at the applied potential of interest, emersed, and then immediately transferred to the vacuum system of the XPS. The elapsed time from electrolyte solution to ultrahigh vacuum was <5 min. Narrow scan XP spectra of the Au (4f) region for wire arrays equilibrated at 0.0 V (Figure 2b) show a single Au (4f) oxidation state (spin−orbit splitting of the Au (4f) region results in a doublet with a ΔeV of 3.67 eV)[29] with a binding energy of 84.0 eV that is consistent with clean, elemental gold.[30] A single Au component remains at potentials up to 0.7 V. Wires equilibrated at higher potentials, from 0.8 to 1.1 V (Figure 2c), show, in addition to the elemental reduced Au component, a prominent shoulder on the high energy side of the peak. This high energy component is assigned to the formation of a Au oxide layer. The chemical shift of this new component, from deconvolution peak fitting, is 85.6 ± 0.1 eV. No significant variation in the chemical shift of this oxide component was seen over the voltage range from 0.8 to 1.1 V. This shoulder is similar in terms of intensity and binding energy to the shoulder seen by Bonzel et al.[3] for macroscopic gold sufaces equilibrated at potentials in this same range, which is to say this chemical shift is not positive enough to be assigned to Au_2O_3 ($4f_{7/2} \approx 85.9$ eV).[31] Therefore the assignment of this species by Bonzel[3] and others[28] to $Au(OH)_3$ is consistent with the spectra of Figure 2c. The ratio between the XPS signal attributable to oxide and that assigned to elemental gold is plotted as a function of potential in Figure 2d. On the basis of the layered oxide structure model suggested by Bando et al.[32] and the inelastic mean free path of the photoelectrons[33] (photoelectrons collected here had an energy of 1170 eV), we estimate that approximately 0.8 monolayers of oxide, corresponding to ≈3.3 Å, is present on the gold surface at +1.1 V vs MSE.

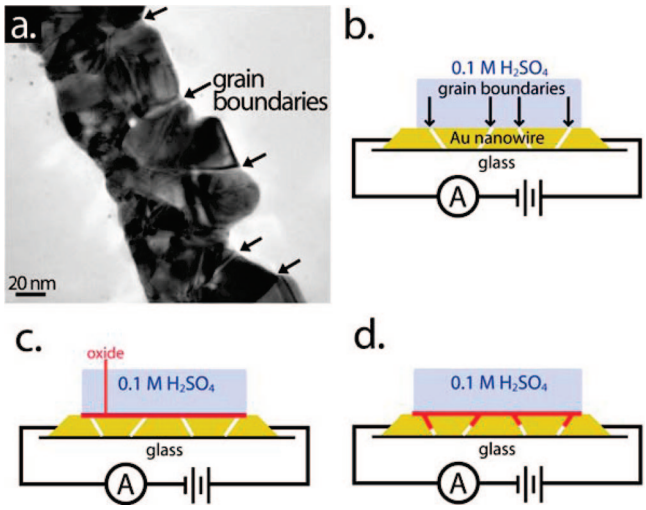

Figure 5. (a) Transmission electron microscopy image of a gold nanowire prepared by LPNE and transferred to a copper grid. Arrows indicate the intersection of grain boundaries with the wire edge. The mean grain diameter is 70−80 nm. (b) Schematic diagram of a polycrystalline gold nanowire in sulfuric acid showing grain boundaries. Oxidation of the nanowire can be limited to the exterior surfaces of the gold nanowire (c) or, in principle, the oxidation can penetrate into grain boundaries as shown in (d), impeding electrical conduction in the nanowire.

The resistance of single gold nanowires supported on glass was measured using an evaporated gold four-point probe (Figure 3a). The evaporated probe and the nanowire were then covered with a poly(methyl methacrylate) (PMMA) resist layer 400 nm in thickness, and a rectangular window of length 46 μm was cut into this resist layer using an electron beam thereby exposing a section of the nanowire through the PMMA resist layer (Figure 3b−d). This device was immersed in 0.10 M H_2SO_4, and the potential of the nanowire versus the MSE reference electrode was controlled versus an MSE using a three-electrode potentiostat. In a typical experiment, the nanowire was first equilibrated at +0.1 V, the potentiostat was disconnected, and the resistance of the nanowire was measured using a Keithley Source Meter 2400 for a period of 30 s during which the resistance stabilized at a new value, the final value of R was recorded, the potentiostat was reconnected, and the process was repeated at a new potential. A plot of wire resistance versus potential obtained using this procedure is shown in Figure 4a for a nanowire with dimensions of 145 nm × 40 nm. The oxidation of the nanowire, commencing at +0.70 V (Figure 1a), progressively increases the measured resistance until at a potential of +1.1 V the resistance is higher by 30% as compared with the reduced state of the wire at +0.1 V. Stepping the potential back in the negative direction, no significant change in the wire resistance is seen until +0.55 V which corresponds to the potential at which the reduction of the oxide commences (Figure 1a). A rapid reduction in resistance is then observed until at +0.40 V, the lower resistance characteristic of the reduced state of the nanowire—prior to oxidation—is nearly recovered. However the new resistance of the nanowire is always slightly higher than the initial state prior to oxidation, and this disparity suggests that some gold has been removed by dissolution. Assuming dissolution is the origin of this resistance change, the quantity of gold removed is 0.4 ± 0.2 gold monolayers per oxidation cycle.

The forward or oxidation scan is shown in Figure 4b for five other nanowires with heights (the smallest dimension) that were both larger and smaller than the wire probed in Figure 4a, ranging from 63 to 18 nm. It is apparent that the increase in resistance seen in Figure 4a is even more pronounced for nanowires with a smaller height dimension. In fact, the relative increase in the resistance, $\Delta R/R_{red}$, increases linearly with diminishing wire height for all of these six nanowires (Figure 4c) with the 18 nm sample producing a $\Delta R/R_{red}$ of 57% at +1.1 V and 70% at +1.2 V (Table 1).

The increase in resistance induced by oxidation is much larger than that which can be explained by the two effects discussed above (Table 1). For the 18 nm height nanowire, for example, the reduction of the wire diameter should induce a $\Delta R/R_{red}$ of ≈4% (column D) whereas a depression in the value of p from 0.38 to 0.0—corresponding to purely diffuse surface scattering, a worst case scenario—would cause a $\Delta R/R_{p=0.38}$ of just 8% (column E). Together, these two mechanisms produce a net $\Delta R/R = 12\%$, well below the experimentally observed value of 57% (column F). A similar relative disparity is seen for all of the six wires probed in this study with the experimentally measured $\Delta R/R$ exceeding the net calculated value by an average of 370%. We conclude that some other mechanism must operate to increase the resistance of these gold nanowires during the oxidation process.

In absolute terms, the excess resistance imposed by an oxide monolayer increases with diminishing wire thickness, and this suggests that the new dissipation mechanism is associated with the wire surface. We hypothesize that this mechanism involves the infiltration of oxide into the grain boundaries of the nanowire at its surfaces, as shown schematically in Figure 5. Unfortunately, direct experimental evidence for this mechanism is elusive: For the polycrystalline gold nanowires investigated here, transmission electron micrographs show a mean grain size measured along the axis of these wires of ≈70 nm (Figure 5a)[25] but we have not been able to directly observe the infiltration of oxide in images such as these. Since the $Au(OH)_3$ produced by oxidation is thermodyamically unstable with respect to decomposition to elemental gold,[1] this may not be surprising.

If segments of grain boundaries *are* oxidized, this can quantitatively account for the anomalous resistance increase documented in Figure 4c as follows: If we suppose that segments of oxide-infiltrated grain boundary have a reflection coefficient, R_c, approaching 1.0, then the effective reflection coefficient, $R_{c,\,eff}$ averaged over the entire nanowire will be in the range from 0.848 (the value characteristic of reduced grain boundaries)[25] and 1.0 (oxidized grain boundaries). By increase of $R_{c,\,eff}$ from 0.848 to larger values within this range (column G, Table 1), the experimentally observed resistance of the oxidized nanowires (column C) can be obtained for all six samples. To first order, this $R_{c,\,eff}$ is a weighted average of the R_c contributed by oxidized regions of grain boundaries adjoining the wire surface, and reduced regions located

deeper within the nanowire: $R_{c,eff} = (1 - x)0.848 + (x)1.00$ where x is the fraction of the wire height into which oxide has infiltrated, on average (column H). The depth of penetration of the oxide into the nanowire at its surface is then the product of x and the wire height, tabulated in column I of Table 1. The oxide infiltration depth calculated in this way is uncorrelated with wire height, varying from 5.8 to 8.4 nm, and this is qualitatively what would be expected for this process, if it is occurring.

In summary, the electrical resistance of gold nanowires measured in situ in dilute sulfuric acid increases in concert with the formation of an oxide monolayer by electrooxidation. The magnitude of the resistance increase is as large as +70% in gold nanowires with lateral dimensions of 18 × 95 nm, much larger than can be explained by the known mechanisms of dissipation in metals. The infiltration of oxide into the grain boundaries at the surface of these nanowires provides a physically reasonable explanation for this anomolous resistance increase, but this mechanism is not confirmed by any direct experimental evidence.

Acknowledgment. This work was supported by the National Science Foundation Grant CHE-0641169 (R.M.P.), the Petroleum Research Fund of the American Chemical Society 46815-AC 10 (R.M.P.), the DOE Office of Basic Energy Sciences DE-FG02-96ER45576 (J.C.H.), and the UCI School of Physical Sciences Center for Solar Energy (R.M.P. and J.C.H.). A.G.G. gratefully acknowledges economic support from the Department of Universities, Research and Information Society (DURSI) of the Catalonia Government through the Grant Number 2007-BE-1-00232.

References

(1) Pourbaix, M. *Atlas of electrochemical equilibria in aqueous solutions*, 2nd ed.; National Association of Corrosion Engineers:Houston, TX, 1974.
(2) Bard, A. J.; Faulkner, L. R. *Electrochemical methods: fundamentals and applications*, 2nd ed.; Wiley: New York, 2001.
(3) Peuckert, M.; Coenen, F. P.; Bonzel, H. P. *Surf. Sci.* **1984**, *141*, 515–532.
(4) Kolb, D. M.; McIntyre, J. D. *Surf. Sci.* **1971**, *28*, 321–334.
(5) Horkans, J.; Cahan, B. D.; Yeager, E. *Surf. Sci.* **1974**, *46*, 1–23.
(6) Kim, Y. T.; Collins, R. W.; Vedam, K. *Surf. Sci.* **1990**, *233*, 341–350.
(7) Chopra, K. L.; Randlett, M. R. *J. Appl. Phys.* **1967**, *38*, 3144–3147.
(8) Lucas, M. S. P. *Thin Solid Films* **1971**, *7*, 435–444.
(9) Campbell, D.; Morley, A. *Rep. Prog. Phys.* **1971**, *34*, 283–368.
(10) Ogawa, S. *J. Vac. Sci. Technol.* **1978**, *15*, 363–365.
(11) Marsocci, V. A.; Shue, S. S. *J. Appl. Phys.* **1971**, *42*, 5047–5050.
(12) Dayal, D.; Wissman, P. *Thin Solid Films* **1977**, *44*, 185–191.
(13) Schumacher, D.; D., S. *Surf. Sci.* **1982**, *123*, 384–396.
(14) Chauvineau, J. P.; Marliere, C. *Thin Solid Films* **1985**, *125*, 25–31.
(15) Dayal, D.; Wissman, P. *Vak.-Tech.* **1989**, *38*, 121–133.
(16) Steinlesberger, G.; Engelhardt, M.; Schindler, G.; Steinhogl, W.; von Glasow, A.; Mosig, K.; Bertagnolli, E. *Microelectron. Eng.* **2002**, *64*, 409–416.
(17) Steinhogl, W.; Schindler, G.; Steinlesberger, G.; Engelhardt, M. *Phys. Rev. B* **2002**, *66*, 075414.
(18) Schindler, G.; Steinlesberger, G.; Engelhardt, M.; Steinhogl, W. *Solid-State Electron.* **2003**, *47*, 1233–1236.
(19) Steinhogl, W.; Schindler, G.; Steinlesberger, G.; Traving, M.; Engelhardt, M. *J. Appl. Phys.* **2005**, *97*, 023706.
(20) Steinhogl, W.; Steinlesberger, G.; Perrin, M.; Scheinbacher, G.; Schindler, G.; Traving, M.; Engelhardt, M. *Microelectron. Eng.* **2005**, *82*, 266–272.
(21) Fuchs, K. *Proc. Cambridge Philos. Soc.* **1938**, *34*, 100–108.
(22) Sondheimer, E. H. *Adv. Phys.* **1952**, *1*, 1–42.
(23) Mayadas, A. F.; Shatzkes, M. *Phys. Rev. B* **1970**, *1*, 1382–1389.
(24) Devries, J. W. C. *Thin Solid Films* **1988**, *167*, 25–32.
(25) Xiang, C.; Kung, S. C.; Taggart, D.; Yang, F.; Thompson, M. A.; Güell, A. G.; Yang, Y.; Penner, R. M. *ACS Nano* **2008**, 10.1021/nn800394k.
(26) Menke, E. J.; Thompson, M. A.; Xiang, C.; Yang, L. C.; Penner, R. M. *Nat. Mater.* **2006**, *5*, 914–919.
(27) Angersteinkozlowska, H.; Conway, B. E.; Hamelin, A.; Stoicoviciu, L. *Electrochim. Acta* **1986**, *31*, 1051–1061.
(28) Juodkazis, K.; Juodkazyte, J.; Jasulaitiene, V.; Lukinskas, A.; Sebeka, B. *Electrochem. Commun.* **2000**, *2*, 503–507.
(29) Moulder, J. F. *Handbook of x-ray photoelectron spectroscopy: a reference book of standard spectra for identification*; Physical Electronics: Eden Prairie, MN, 1995.
(30) Seah, M. P.; Smith, G. C.; Anthony, M. T. *Surf. Interface Anal.* **1990**, *15*, 293–308.
(31) Pireaux, J. J.; Liehr, M.; Thirty, P. A.; Delrue, J. P.; Caudano, R. *Surf. Sci.* **1984**, *141*, 221–232.
(32) Bando, H.; Koizumi, K.; Oikawa, Y.; Daikohara, K.; Kulbachinskii, V.; Ozaki, H. *J. Phys.: Condens. Matter* **2000**, *12*, 5607–5616.
(33) Powell, C. J.; Jablonski, A. *NIST Electron Inelastic-Mean-Free-Path Database*, Version *1.1* ed.; National Institute of Standards and Technology: Gaithersburg, MD, 2000.

NL8021175